Recurrence analysis of strange nonchaotic dynamics

E. J. Ngamga,[1] A. Nandi,[2] R. Ramaswamy,[2] M. C. Romano,[1] M. Thiel,[1] and J. Kurths[1]
[1]*Nonlinear Dynamics Group, Institute of Physics, University of Potsdam, Potsdam 14415, Germany*
[2]*School of Physical Sciences, Jawaharlal Nehru University, New Delhi 110 067, India*
(Received 11 December 2006; published 29 March 2007)

We present methods to detect the transitions from quasiperiodic to chaotic motion via strange nonchaotic attractors (SNAs). These procedures are based on the time needed by the system to recur to a previously visited state and a quantification of the synchronization of trajectories on SNAs. The applicability of these techniques is demonstrated by detecting the transition to SNAs or the transition from SNAs to chaos in representative quasiperiodically forced discrete maps. The fractalization transition to SNAs—for which most existing diagnostics are inadequate—is clearly detected by recurrence analysis. These methods are robust to additive noise, and thus can be used in analyzing experimental time series.

DOI: 10.1103/PhysRevE.75.036222 PACS number(s): 82.40.Bj, 83.85.Ns

I. INTRODUCTION

Starting with the seminal works of Landau [1] and Ruelle and Takens [2], the transition from regular to chaotic dynamics via quasiperiodicity has attracted great interest. Different aspects of this transition have been studied both theoretically and experimentally over the past decades. About two decades ago, however, it was found that in quasiperiodically forced systems the transition to chaos is generally mediated by strange nonchaotic attractors (SNAs). SNAs were first described by Grebogi *et al.* in 1984 [3] and since then have been investigated in a number of numerical [4–14], experimental [15,16], and mathematical [17–20] studies. These unusual attractors are thought to be important in biological systems [10,21] and in nonlinear dynamics based communication [22,23].

SNAs are geometrically strange (or fractal) while they are nonchaotic in the dynamical sense. These attractors can be regarded as intermediate between regularity and chaos. Typical trajectories experience arbitrarily long time intervals of expansion while on average, contraction dominates. This behavior yields a strange geometric structure in the phase space similar to chaotic attractors. Different routes to SNAs have been reported: (i) collision between a period-doubled torus and its unstable parent [7], (ii) fractalization of a torus [12], (iii) blowout bifurcation [24], and (iv) intermittency [13]. Most studies on SNAs have focused on their characterization using tools such as Lyapunov exponents and their variance, spectral properties [4,5], geometrical properties [6,10], local divergence of trajectory [25], phase sensitivity and rational approximations [8], functional maps and invariant curves [12,26], as well as a renormalization-group analysis [27].

In the present work, we propose measures of complexity which are based on the *recurrences* of states in phase space to detect transitions from regular to chaotic motion via SNAs. Moreover, they enable us to identify the birth of an SNA for the fractalization route, which is not always apparent in measures based on the Lyapunov exponents. We further show that recurrence based measures are robust with respect to additive noise, and are therefore highly suitable for the analysis of experiments [28] where the data may be both noisy and sparse.

The paper is organized as follows. In Sec. II, we define the recurrence measures and apply them in Sec. III for the detection of some routes to SNAs in discrete one-dimensional nonlinear mappings. Section IV examines the fractalization of a torus to an SNA, and Sec. V the transition from SNAs to chaos. The final section summarizes our results.

II. MEASURES OF COMPLEXITY

The concept of recurrences in dynamical systems goes back to Poincaré [29], who has shown that under certain conditions, the orbit of a bounded dynamical system must return arbitrarily close to each former point of its route with probability one. The time of return can, however, be arbitrarily long. A visual representation of such recurrences is provided by recurrence plots (RPs), which were introduced in 1987 [30]. RPs are defined for a given trajectory $\{\vec{\mathbf{x}}_i\}_{i=1}^N$, of a dynamical system, where $\vec{\mathbf{x}}_i \in \mathbb{R}^n$. They are based on the matrix

$$R_{i,j} = \Theta(\delta - \|\vec{\mathbf{x}}_i - \vec{\mathbf{x}}_j\|), \quad i,j = 1, \ldots, N, \tag{1}$$

where δ is a predefined threshold, $\Theta(\cdot)$ the Heaviside function, and $\|\cdot\|$ denotes a norm. In this paper we use the maximum norm, also called infinity norm, which is given by $\|\vec{x}_i\|_\infty = \max(|x_i^1|, |x_i^2|, \ldots, |x_i^d|)$ where $|x_i^j|$ denotes the jth component of the vector $\vec{x}_i$ and d is the dimension of the phase space. For computing RPs, the maximum norm is often used because it is computationally faster and its independence from the phase space dimension is of relevance if in one analysis different embeddings of a time series have to be used. Points that are closer (further) than δ yield an entry "1" ("0") in the matrix $R_{i,j}$. Then, the values "1" and "0" are depicted as black and white dots in a two-dimensional plot, providing a visual representation of the system dynamics.

Special attention has to be paid to the choice of the threshold δ. It is desirable that the smallest threshold possible is chosen. However, in the presence of noise a larger threshold might be needed because noise would distort any existing structure in the RP. It has been suggested that this threshold should range from a few percent of the maximum

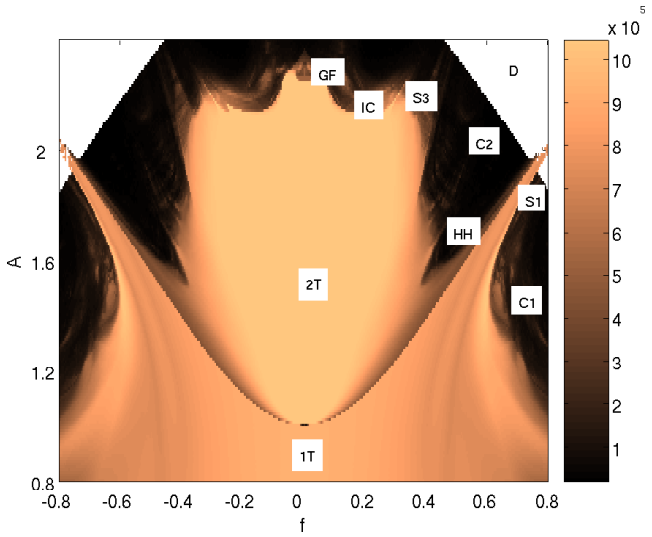

FIG. 1. (Color online) Phase diagram of the quasiperiodically forced cubic map [Eq. (9)], obtained using N_{MPRT} [Eq. (3)]. 1T and 2T correspond to tori of period 1 and 2, respectively. GF corresponds to the region where the gradual fractalization of the torus occurs. HH represents the region where the SNA is created through the Heagy Hammel route. S1 and S3 denote regions where the SNA appears through type-I and type-III intermittencies, respectively. IC denotes the region where SNAs are created through crisis-induced intermittency. C1 and C2 correspond to chaotic regions. For the parameter values in the region marked D, the trajectories escape to infinity.

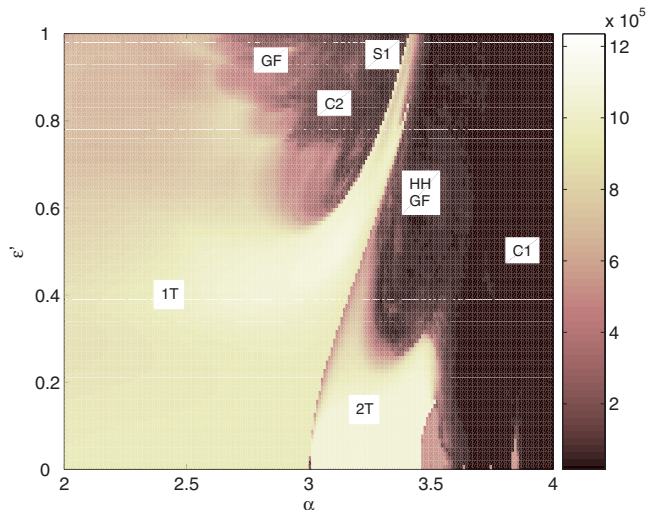

FIG. 2. (Color online) Phase diagram of the quasiperiodically forced logistic map [Eq. (8)], obtained using N_{MPRT} [Eq. (3)].

phase space diameter [31] and should not exceed 10% of the mean [32]. In the presence of observational noise, the choice $\delta=5\sigma$, with σ being the standard deviation of the observational noise, has been shown to be more appropriate [33]. We use this latter choice.

Several measures have been proposed to quantify the structures in RPs, which have found applications in the analysis of, e.g., physiological or geophysical time series [34–36]. It has been shown that—under some conditions—all topological information about the underlying system is contained in the RP [37]. In [38] it has been shown that the recurrence time statistics corresponding to white vertical structures in the RP are directly related to the information dimension. These statistics seem to be of special importance in the present study. Marwan *et al.* [39] have proposed further measures of complexity to quantify vertical black structures in RPs: this permits the identification of chaos-chaos transitions.

In order to detect transitions from a torus to an SNA, we extend this approach to the "white vertical lines" in RPs. Note that the length of these lines is equal to the time needed by the system to recur to a previously visited state. Here we propose two types of recurrence analysis in order to identify transitions to or from SNAs.

(1) Transition from a torus to an SNA. From the RP, we evaluate the frequency distribution $P(w)$ of the lengths w of the white vertical lines. We then compute the *mean recurrence time* (T_{MRT}) from this distribution,

$$T_{MRT} = \sum_{w=1}^{N} wP(w) \Big/ \sum_{w=1}^{N} P(w). \tag{2}$$

Furthermore, we determine the *number of recurrence* of the most probable recurrence time (N_{MPRT}). It indicates how many times the system has recurred using the most probable recurrence time and is given by

$$N_{MPRT} = \max(\{P(w)\}; w = 1, \ldots, N). \tag{3}$$

Contrary to the definitions of measures based on black vertical lines, we consider $w_{min}=1$ in order to estimate the mean recurrence times, because we are interested in all time spans between each recurrences, and a vertical white gap between two recurrence points, even if only $w=1$, corresponds to the time span between a recurrence. We also consider the variance σ_{MRT} of T_{MRT} and σ_{MPRT} of N_{MPRT}. For a given sufficiently long trajectory, the variance is evaluated by dividing the trajectory into k segments and computing T_{MRT} and N_{MPRT} for each segment separately. Thus

$$\sigma_{MRT} = \frac{1}{k-1} \sum_{l=1}^{k} [T_{MRT}(l) - \bar{T}_{MRT}]^2, \tag{4}$$

$$\sigma_{MPRT} = \frac{1}{k-1} \sum_{l=1}^{k} [N_{MPRT}(l) - \bar{N}_{MPRT}]^2, \tag{5}$$

where the overbar indicates the mean value.

(2) Transition from SNAs to chaos. To detect this transition [40] we use the fact that two trajectories in the SNA regime starting at different initial conditions but driven by the same quasiperiodic force with an identical phase synchronize, whereas in the chaotic regime, they do not [22]. In order to quantify synchronization, we compute first the cross-recurrence matrix (CRM)

$$CR_{i,j}^{m,\delta} = \Theta(\delta - \|\vec{\mathbf{x}}_i - \vec{\mathbf{y}}_j\|) \tag{6}$$

of the two separate trajectories $\vec{\mathbf{x}}_i$ and $\vec{\mathbf{y}}_j$, $i,j=1,\ldots,N$. The trajectories are reconstructed by delay coordinates and m denotes the embedding dimension. The threshold δ is taken in units of the average standard deviation σ of the two time series. As in other computations, we set the delay to 1. If

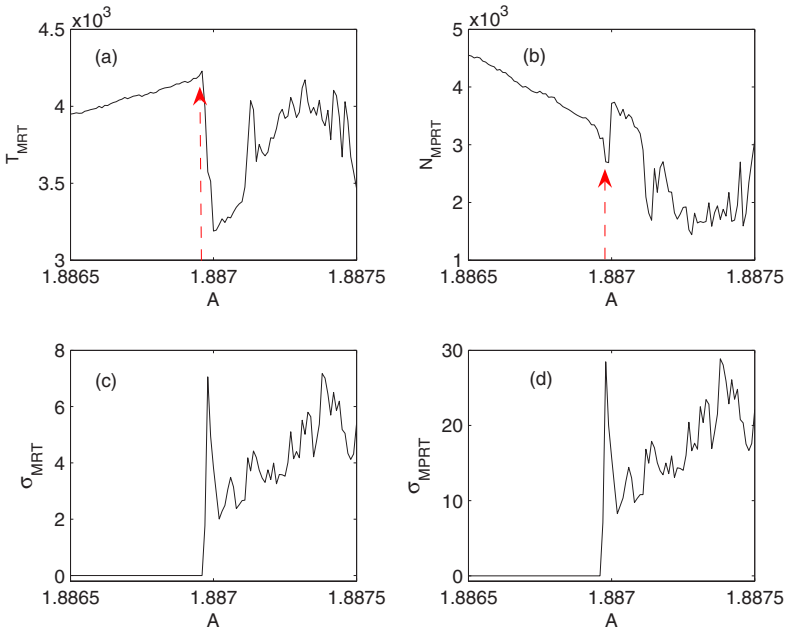

FIG. 3. (Color online) Transition from a doubled torus to SNA through a HH mechanism in the cubic map [Eq. (9)]. (a) behavior of T_{MRT}; (b) behavior of N_{MPRT}; (c) variance of T_{MRT}; and (d) variance of N_{MPRT}. The critical value is $A \approx 1.886\,97$.

both trajectories synchronize, the main diagonal of the cross-recurrence plot (CRP) [41] will be continuous, otherwise the main diagonal will be interrupted. We then compute the *determinism* (D_{ET}) [37] of the main diagonal line,

$$D_{ET} = \sum_{l=l_{min}}^{N} lD(l) \Big/ \sum_{l=1}^{N} lD(l), \tag{7}$$

where $D(l)$ denotes the frequency distribution of the length l of black diagonal lines. Note that in this case D_{ET} is computed only on the main diagonal, i.e., only for coordinates $i=j$. If both systems $\vec{\mathbf{x}}_i$ and $\vec{\mathbf{y}}_j$ are synchronized, $D_{ET}=1$, otherwise $D_{ET}<1$. Therefore by computing D_{ET} in dependence on the bifurcation parameter, we can detect the transition from SNAs to chaotic attractors.

III. THE TRANSITION FROM QUASIPERIODIC DYNAMICS TO SNAS

We next study the transition from quasiperiodic dynamics to SNAs in the quasiperiodically forced logistic map [42],

$$x_{n+1} = \alpha[1 + \varepsilon \cos(2\pi\theta_n)]x_n(1 - x_n),$$

$$\theta_{i+1} = \theta_i + \omega \bmod 1 \tag{8}$$

and the quasiperiodically forced cubic map [43],

$$x_{i+1} = Q + f\cos(2\pi\theta_i) - Ax_i + x_i^3,$$

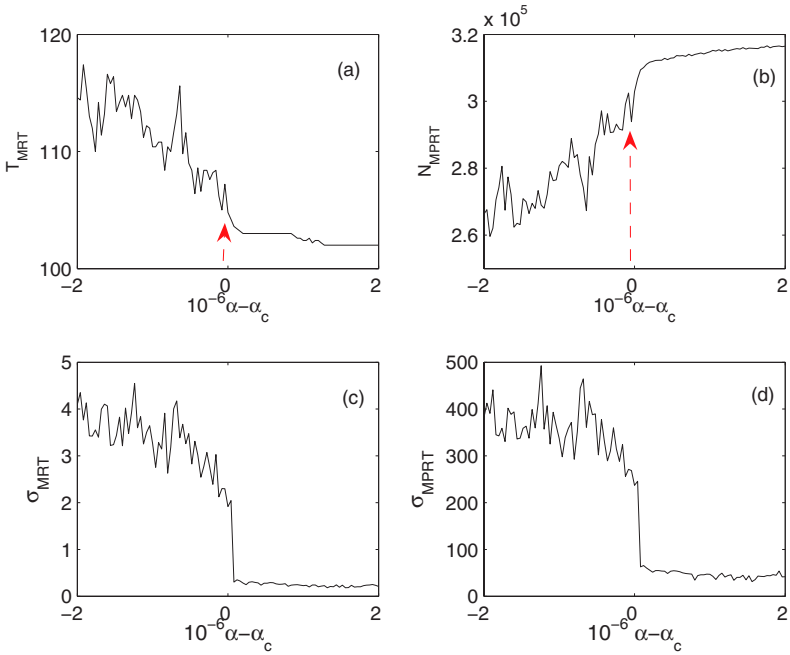

FIG. 4. (Color online) Type-I intermittency route in the logistic map [Eq. (8)]. (a) Behavior of T_{MRT}; (b) behavior of N_{MPRT}; (c) variance of T_{MRT}; and (d) variance of N_{MPRT}. The critical value is $\alpha_c \approx 3.405\,808\,8$.

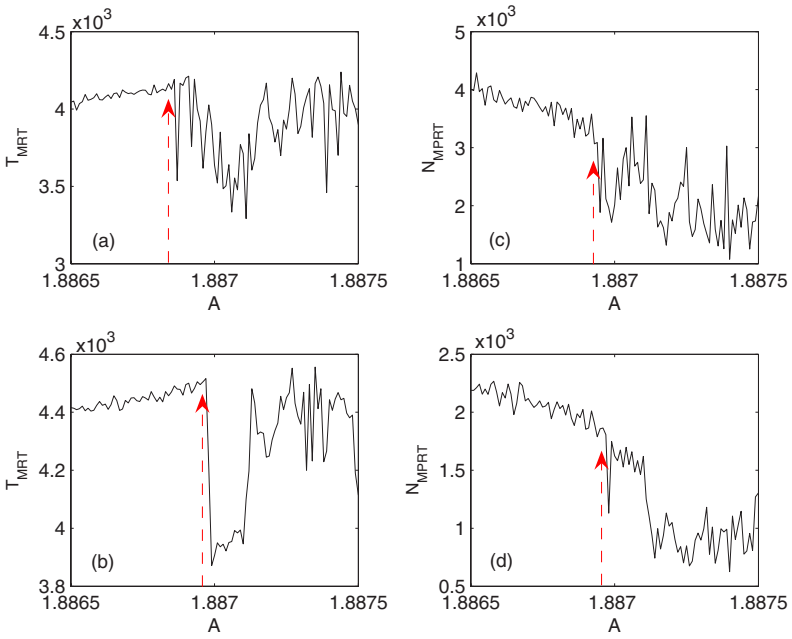

FIG. 5. (Color online) Robustness of the recurrence time measures against noise for the HH route in the cubic map [Eq. (9)]. (a) and (c) T_{MRT} and N_{MPRT} for dynamical noise of amplitude 10^{-4}; and (b) and (d) T_{MRT} and N_{MPRT} for observational noise of amplitude 0.01. The threshold used $\delta=0.001$ and $N=10\,000$ normalized data points.

$$\theta_{i+1} = \theta_i + \omega \bmod 1. \tag{9}$$

These systems have been already investigated and various transitions to SNAs have been identified using tools such as Lyapunov exponents and their variance, as well as finite-time Lyapunov exponents, dimensions, power spectral measures, and phase sensitivity exponents [42,43]. Using N_{MPRT} [Eq. (3)], we obtain for the logistic and cubic maps two-parameter [(ε', α) and (A, f), respectively] phase diagrams which clearly show transitions in the dynamics that are in strong agreement with those reported in [42,43]. These phase diagrams were computed using $\delta=0.06$ and $N=10\,000$ normalized data points. The parameter $\varepsilon'=\varepsilon/(4/\alpha-1)$ is a rescaled driving parameter.

The phase diagram of the cubic map [43] is given in Fig. 1. It can be observed that the dynamics is symmetric about $f=0$, with two chaotic regions C1 and C2. Bordering these chaotic areas, one finds SNAs which are created through different mechanisms such as Heagy Hammel (HH), gradual fractalization (GF), intermittencies of type-I and type-III (S1, S3), and interior crisis (IC). There are also regions where the dynamics is on quasiperiodic attractors of period 1 and 2 which are marked, respectively, by 1T and 2T. The phase diagram of the quasiperiodically forced logistic map [42] obtained using N_{MPRT} exhibits very interesting patterns (Fig. 2). Almost all the transitions found in the phase diagram of the cubic map are also present here.

In order to exemplify the performance of T_{MRT} and N_{MPRT}, we analyze in detail two typical transitions to SNAs.

(i) The Heagy Hammel route (HH) in the cubic map [Eq. (9)]. In this route to SNAs, the birth of a SNA is due to the collision between a period-doubled torus with its unstable parent [7]. We fix the bifurcation parameter $f=0.7$ and vary A in the range $1.8865 \leqslant A \leqslant 1.8875$. At the starting value of A, we have a period-doubled torus of period 2. As A increases to the value 1.8868, the torus begins to wrinkle and approaches its parent, with which it collides and ultimately gives birth to a fractal attractor when A is increased up to the value 1.886 97. It has been shown that at this value of A, the attractor possesses a geometrically strange structure and is nonchaotic [43]. Using the threshold $\delta=0.001$ and $N=10\,000$ normalized data points for the computation of the RP, T_{MRT} and N_{MPRT} are able to detect the critical value $A=1.886\,97$ at which both tori collide [Figs. 3(a) and 3(b)]. The variances σ_{MRT} and σ_{MPRT}, computed using $N=300\,000$ data points for the whole trajectory and $N=2\,000$ data points for each segment, show this transition even more clearly [Figs. 3(c) and 3(d)]. One can see that the recurrence time measures vary slightly before the collision and at the critical value there is a drastic jump, after which some oscillations start indicating an irregular behavior.

(ii) The intermittency route (S1) wherein a strange attractor disappears and is replaced by a one-frequency torus through an analog of the saddle-node bifurcation. In the vicinity of this phenomenon the attractor is strange and nonchaotic. It has been shown that the dynamics at this transition is intermittent, and the scaling behavior is characteristic of type-I intermittency [13,44]. In the logistic map [Eq. (8)], this intermittency route to SNAs (denoted S1) occurs along the right edge of the chaotic region C2 in Fig. 2. For $\varepsilon'=1$ and varying α, we see in Fig. 4 that the measures T_{MRT} and N_{MPRT} fluctuate rather strongly in the SNA regime and smoothly in the quasiperiodic one. There is an abrupt change at the critical value $\alpha_c \approx 3.405\,808\,8$ where the intermittent transition takes place. The threshold is set to $\delta=0.03$. For the computation we have used $N=10\,000$ normalized data points for N_{MPRT} and T_{MRT}, $N=300\,000$ for the variances, and $N=2000$ as the length of each segment.

We have also identified by these measures other transitions to SNAs in [42,43]. Indeed, all four measures based on RPs are able to detect these transitions to SNAs. Since the mechanism for the creation of SNAs is different for each route, it was not easy to find a satisfactory threshold for the computation of the RP which holds for all the different routes to SNAs. However, for each route to SNAs, we are able to find a threshold which leads to a good detection

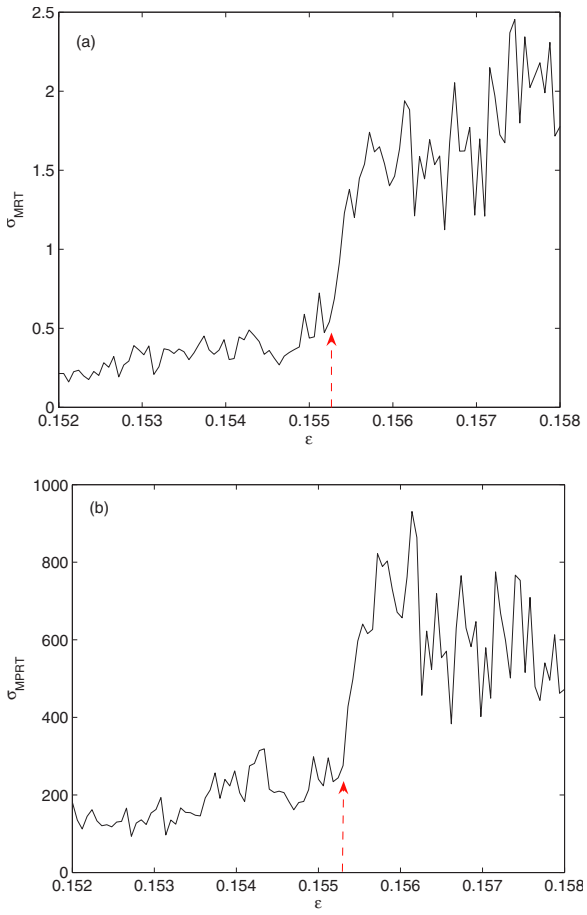

FIG. 6. (Color online) Fractalization route in the logistic map [Eq. (10)]. (a) Variance of T_{MRT} and (b) Variance of N_{MPRT}; variances computed using $\delta=0.05$, $N=750\,000$ data points as the whole trajectory and $N=3000$ as the length of each segment. The critical value of the bifurcation parameter is $\varepsilon_c \approx 0.1553$.

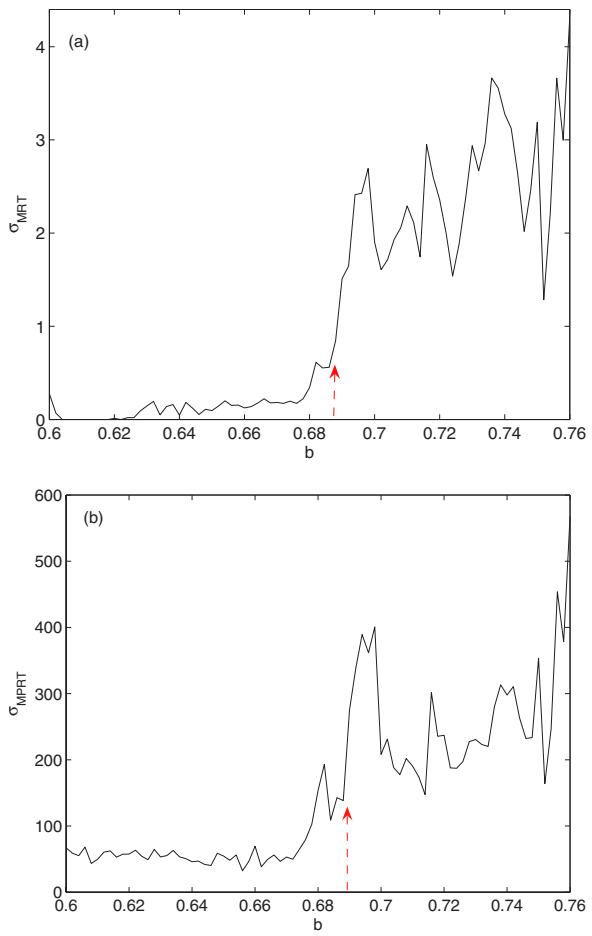

FIG. 7. (Color online) Fractalization route in the Hénon map [Eq. (11)]. (a) Variance of T_{MRT} and (b) variance of N_{MPRT}. Variances computed using $\delta=0.05, 750\,000$ data points and 2500 as the length of each segment. The variances increase suddenly at the bifurcation parameter $b \approx 0.69$.

of the transition to SNAs by the recurrence time measures.

The robustness of the measures against noise has also been investigated. It is known that noise generally decreases the threshold for chaos since transitions and bifurcations get blurred in the presence of fluctuations. We present here the case of the HH route in the cubic map [Eq. (9)]. Figures 5(a) and 5(c) show T_{MRT} and N_{MPRT} when weak dynamical uniformly distributed noise of amplitude 10^{-4} has been added to the variable x (in order to keep the quasiperiodicity of the forcing). Figures 5(b) and 5(d) represent the case of observational uniformly distributed noise of amplitude 0.01. The transition from torus to SNAs globally survives. In the case of dynamical noise and especially for T_{MRT} [Fig. 5(a)], noise has considerably reduced the value of the bifurcation parameter at which the transition to SNAs appears, but the recurrence time measures are still able to detect the transition.

IV. FRACTALIZATION ROUTE TO SNA

The fractalization of a torus is both the most common and the most intriguing transition to SNAs. In this mechanism, a torus becomes more and more wrinkled as the forcing increases until it breaks up to form a strange set. The fractalization appears as a gradual change in the structure of the attractor which is difficult to relate to a precise bifurcation point, where a sudden change in the dynamics occurs due to the crossing of a well-defined critical threshold. In some particular cases, namely for forced noninvertible maps, it is possible to define a critical threshold for the fractalization transition. In contrast to other mechanisms for the emergence of SNAs, there is no obvious unstable set involved in the fractalization route. Datta *et al.* [46] have, however, recently used techniques introduced by Kim *et al.* [47] to find unstable sets for the fractalization process using a sequence of rational approximations of the irrational forcing. They found that these unstable sets are created through a cascade of period-doubling bifurcations and collision of chaotic bands with them. This causes a cascade of interior merging crises whereby the fractalization process takes place.

The first example we study is the fractalization route in the forced logistic map as described by Nishikawa and Kaneko [12]:

$$x_{n+1} = a x_n (1 - x_n) + \varepsilon \sin(2\pi\theta_n),$$

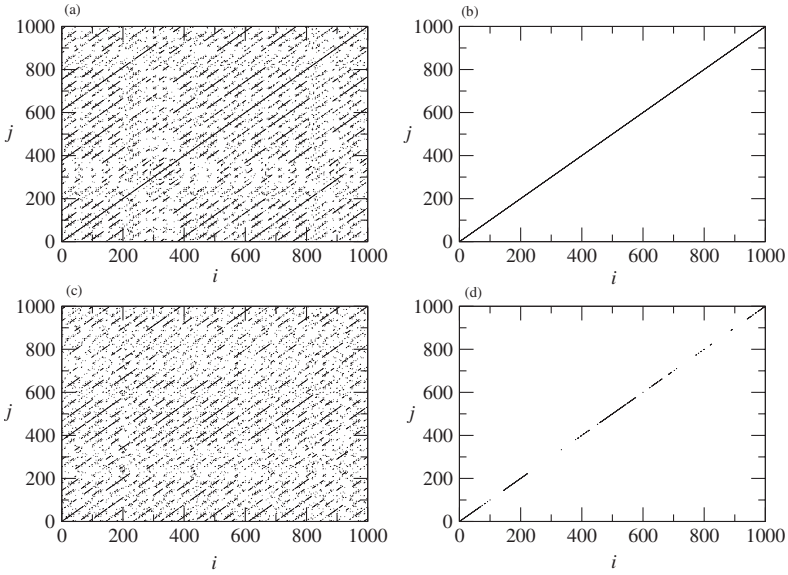

FIG. 8. CRP of the forced logistic map [Eq. (8)]: (a) in the SNA regime with $\alpha=3.32$, $\varepsilon'=0.595$, and (c) in the chaotic regime with $\alpha=3.33$, $\varepsilon'=0.595$. Due to synchronization, the CRP and the ordinary RP are identical in the SNA regime, whereas this is not the case in the chaotic regime. In (b) and (d) only the main diagonals for the SNAs and chaotic attractors are shown. The threshold for the computation of the CRP is $\delta=0.2\sigma$ where σ is the average of the individual standard deviations of the two time series. The embedding dimension is taken to be $m=3$.

$$\theta_{n+1} = \theta_n + \omega \bmod 1. \tag{10}$$

We fix $a=3$ and vary ε. At $\varepsilon=0$, the attractor of the system is a straight-line torus. As ε is increased, oscillations of the torus start to appear and it becomes fractal at $\varepsilon \approx 0.1553$. The variances σ_{MRT} and σ_{MPRT} vary slightly but at the critical value $\varepsilon_c \approx 0.1553$, they suddenly increase and their fluctuations become larger for the following values of the bifurcation parameter (Fig. 6).

A second example that we consider is the fractalization route in the Hénon map [45], given by the equations

$$u_{n+1} = 1 + v_n - bu_n^2 + A\cos(2\pi\theta_n),$$

$$u_{n+1} = cu_n,$$

$$\theta_{n+1} = \theta_n + \omega \bmod 1, \tag{11}$$

with $c=0.1$ and $A=0.7$. The bifurcation parameter is b. Sosnovtseva *et al.* [45] have found that the transition to SNAs happens at $b=0.7$; we rather find the transition closer to 0.69, where an abrupt increase of σ_{MRT} and σ_{MPRT} can be observed (see Fig. 7).

V. THE TRANSITION FROM SNAS TO CHAOTIC ATTRACTORS

The transition from SNAs to chaotic attractors is a purely dynamical one: the structure of the attractor remains essentially unchanged, while the largest Lyapunov exponent becomes positive. This is a consequence of the manner in which the invariant measure is redistributed on the attractor [48]. Since the largest Lyapunov exponent of SNAs is negative, two such systems are able to undergo complete synchronization. It has been shown in [22] that regardless of the initial conditions of two identical SNAs, they eventually converge to the same dynamics if the phase of the quasiperiodic driving coincides for both of them. In contrast, in the chaotic regime, both systems have positive Lyapunov exponents, and therefore they cannot synchronize. A recurrence measure, which can easily identify the synchronization, and hence the

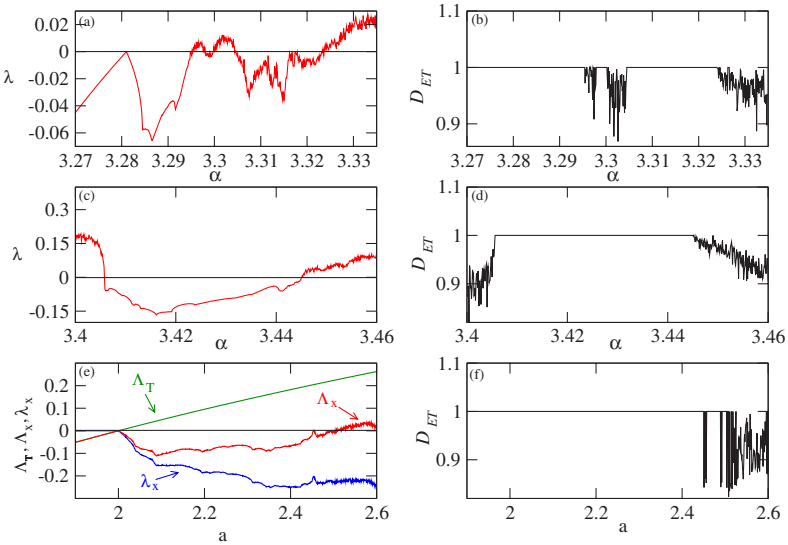

FIG. 9. (Color online) Comparison of the Lyapunov exponent (λ) and D_{ET} for the CRPs on the main diagonal line. (a) λ for Eq. (8) with $\varepsilon'=0.595$, (b) the corresponding D_{ET}, (c) λ for Eq. (8) with $\varepsilon'=1$, (d) the corresponding D_{ET}, (e) Λ_T, Λ_x and λ_x for Eq. (12) and (f) the corresponding D_{ET}. A D_{ET} value of unity corresponds to SNAs dynamics, and a drop in the value of D_{ET} to lower values indicates the SNAs to chaos transition. In all cases studied here, we use $\delta=0.2\sigma$ and embedding dimension is $m=3$.

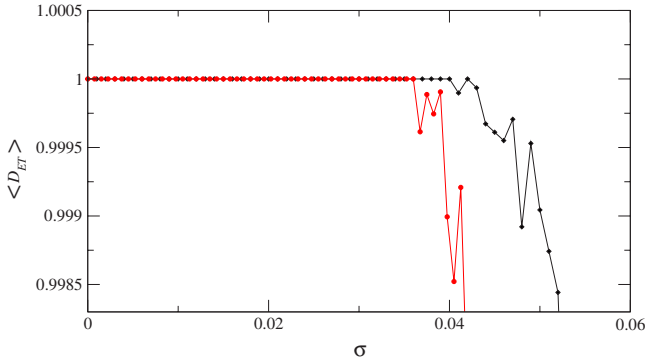

FIG. 10. (Color online) D_{ET} (averaged over 200 stochastic runs) for Eq. (8) with increasing noise amplitude σ. The line with diamonds corresponds to the HH route at $\alpha=3.32$ and $\varepsilon'=0.595$. The line with filled circles corresponds to the intermittency route at $\alpha=3.385$ and $\varepsilon'=0.8$. We use $\delta=0.2\sigma$ and the embedding dimension is $m=3$.

transition from SNAs to chaos, is based on the D_{ET} of the CRM defined in Eq. (6) for two different time series generated by the same initial phase θ_0. If both trajectories synchronize, we obtain an uninterrupted main diagonal in the CRP. Otherwise, the main diagonal is interrupted indicating the chaotic regime. This can be clearly seen in Fig. 8 where the CRPs are illustrated for both cases. Thus by computing the D_{ET} of the CRP only on the main diagonal, the transition from SNAs to chaos can be detected very clearly. In the SNA regime $D_{ET}=1$, while in the chaotic regime $D_{ET}<1$.

The specific characteristics of SNAs depend on the mechanisms through which they were created, and it appears that this feature carries over into the corresponding chaotic attractors. Accordingly, we have numerically examined the SNAs to chaos transition for SNAs created via the HH [7] and intermittency [13] routes in the quasiperiodically forced logistic map [Eq. (8)]. We have also studied the mapping

$$x_{n+1} = (a\cos 2\pi\theta_n + b)\sin 2\pi x_n,$$

$$\theta_{n+1} = \theta_n + \omega \bmod 1, \tag{12}$$

where the blowout bifurcation [24,49] route to SNAs has been observed.

These results are shown in Fig. 9. For the HH route we use $\varepsilon'=0.595$ (see Fig. 2) in the logistic map. Figures 9(a) and 9(b) show the Lyapunov exponent and D_{ET}, respectively. As it can be clearly seen, when the Lyapunov exponent changes from negative to positive, this is accompanied by a sharp drop in the value of D_{ET}. Analogously, for the intermittency route to chaos at $\varepsilon'=1$, the behavior of the Lyapunov exponent and D_{ET} is shown in Figs. 9(c) and 9(d).

In the case of the blowout bifurcation, the largest nontrivial Lyapunov exponent Λ_x is compared to D_{ET} and shows the SNA to chaos transition [see Figs. 9(e) and 9(f)]. Recall that the blowout bifurcation occurs in systems with a symmetric low dimensional invariant subspace S: when the transverse Lyapunov exponent Λ_T goes from negative to positive through zero, the invariant subspace loses its stability, and SNAs can be created if the total Lyapunov exponent Λ_x remains nonpositive. Λ_x is deduced from the transverse Lyapunov exponent Λ_T via [24,49]

$$\Lambda_x = \Lambda_T - |\lambda_x|, \tag{13}$$

where λ_x is the nonzero Lyapunov exponent of Eq. (12).

D_{ET} is found to be robust to added external noise. This is very important in the context of the analysis of experimental data. In Fig. 10, we show the effect of uniform additive noise in Eq. (8) for the HH and the intermittency routes.

VI. SUMMARY

Our main objective in this work has been to use recurrence time statistics in order to detect transitions to or from SNAs. To detect the transition from quasiperiodic motion to SNAs, we have introduced four measures, namely T_{MRT}, N_{MPRT}, and their variances, which are based on the time needed by the system to recur to a neighborhood of a previous point of the trajectory. These measures have been able to detect the onset of the strange nonchaotic dynamic in the Heagy Hammel and intermittency routes, respectively, in the cubic and logistic maps. Moreover, they also detect the fractalization of a torus to an SNA, which is not easily located by the measures based on the Lyapunov exponent [50]. We have seen, for example, in the Heagy Hammel route that these four measures vary slightly in the quasiperiodic regime. At the critical value of the bifurcation parameter, there is a drastic jump followed by irregular fluctuations of the recurrence time measures indicating the SNA regime.

The transition from SNAs to chaos has been identified by computing the determinism of a cross-recurrence plot of two different time-series generated by the same initial phase. At the critical value, we have noticed a sharp change in the value of the determinism from its maximum value 1.

These measures—which are robust against noise—can detect these transitions even when the orbits are not very long, in contrast to Lyapunov exponent based measures. The present measures are also advantageous in the sense that they do not require the knowledge of the equations governing the system under study. Therefore they are very appropriate for the analysis of experimental data. We will show the applicability of these measures for continuous systems and experimental data in a forthcoming paper.

ACKNOWLEDGMENTS

This work was supported by the Deutscher Akademischer Austausch Dienst (E.J.N.), the Promotion Kolleg (E.J.N., M.C.R., J.K.), and SPP1114 (M.T., J.K.). A.N. is supported by the CSIR, India. We thank Awadhesh Prasad and Dr. N. Marwan for very helpful suggestions and discussions.

[1] L. D. Landau, Dokl. Akad. Nauk SSSR **44**, 339 (1944).
[2] D. Ruelle and F. Takens, Commun. Math. Phys. **20**, 167 (1971).
[3] C. Grebogi, E. Ott, S. Pelikan, and J. A. Yorke, Physica D **13**, 261 (1984).
[4] A. Bondeson, E. Ott, and T. M. Antonsen, Phys. Rev. Lett. **55**, 2103 (1985).
[5] F. J. Romeiras and E. Ott, Phys. Rev. A **35**, 4404 (1987).
[6] M. Ding, C. Grebogi, and E. Ott, Phys. Rev. A **39**, 2593 (1989).
[7] J. F. Heagy and S. M. Hammel, Physica D **70**, 140 (1994).
[8] A. Pikovsky and U. Feudel, Chaos **5**, 253 (1995).
[9] U. Feudel, J. Kurths, and A. Pikovsky, Physica D **88**, 176 (1995).
[10] M. Ding and J. Scott Kelso, Int. J. Bifurcation Chaos Appl. Sci. Eng. **4**, 553 (1994).
[11] Y.-C. Lai, Phys. Rev. E **53**, 57 (1996).
[12] T. Nishikawa and K. Kaneko, Phys. Rev. E **54**, 6114 (1996).
[13] A. Prasad, V. Mehra, and R. Ramaswamy, Phys. Rev. Lett. **79**, 4127 (1997).
[14] A. Venkatesan and M. Lakshmanan, Phys. Rev. E **58**, 3008 (1998).
[15] W. L. Ditto *et al.*, Phys. Rev. Lett. **65**, 533 (1990).
[16] T. Zhou, F. Moss, and A. Bulsara, Phys. Rev. A **45**, 5394 (1992).
[17] G. Keller, Fund. Math. **151**, 139 (1996).
[18] J. Stark, Physica D **109**, 163 (1997).
[19] R. Sturman and J. Stark, Nonlinearity **13**, 113 (2000).
[20] B. R. Hunt and E. Ott, Phys. Rev. Lett. **87**, 254101 (2001).
[21] A. Prasad, B. Biswal, and R. Ramaswamy, Phys. Rev. E **68**, 037201 (2003).
[22] R. Ramaswamy, Phys. Rev. E **56**, 7294 (1997).
[23] C.-S. Zhou and T.-L. Chen, Europhys. Lett. **38**, 261 (1997).
[24] T. Yalçinkaya and Y.-C. Lai, Phys. Rev. Lett. **77**, 5039 (1996).
[25] T. Kapitaniak and J. Wojewoda, *Attractors of Quasiperiodically Forced Systems* (World Scientific, Singapore, 1993).
[26] V. S. Anishchenko, T. E. Vadivasova, and O. Sosnovtseva, Phys. Rev. E **53**, 4451 (1996).
[27] U. Feudel, S. Kuznetsov, and A. Pikovsky, *World Scientific Series on Nonlinear Science*, Series A, Vol. 56 (World Scientific, Singapore, 2006).
[28] K. Thamilmaran, D. V. Senthilkumar, A. Venkatesan, and M. Lakshmanan, Phys. Rev. E **74**, 036205 (2006).
[29] H. Poincaré, Acta Math. **13**, 1 (1890).
[30] J. P. Eckmann, S. O. Kamphorst, and D. Ruelle, Europhys. Lett. **4**, 973 (1987).
[31] G. M. Mindlin and R. Gilmore, Physica D **581**, 229 (1992).
[32] J. P. Zbilut and J. R. Webber, Phys. Lett. A **171**, 199 (1992).
[33] M. Thiel, M. C. Romano, J. Kurths, R. Meucci, E. Allaria, and F. T. Arecchi, Physica D **171**, 138 (2002).
[34] C. L. Weber, Jr. and J. P. Zbilut, J. Appl. Physiol. **76**, 965 (1994).
[35] K. Shockley, M. Butwill, J. P. Zbilut, and C. L. Webber, Jr., Phys. Lett. A **305**, 59 (2002).
[36] N. Marwan, M. Thiel, and N. R. Nowaczyk, Nonlinear Processes Geophys. **9**, 325 (2002).
[37] N. Marwan, M. C. Romano, M. Thiel, and J. Kurths, Phys. Rep. **438**, 237 (2007).
[38] J. B. Gao, Phys. Rev. Lett. **83**, 3178 (1999).
[39] N. Marwan, N. Wessel, U. Meyerfeldt, A. Schirdewan, and J. Kurths, Phys. Rev. E **66**, 026702 (2002).
[40] Y. C. Lai, Phys. Rev. E **53**, 57 (1996).
[41] N. Marwan and J. Kurths, Phys. Lett. A **302**, 299 (2002).
[42] A. Prasad, V. Mehra, and R. Ramaswamy, Phys. Rev. E **57**, 1576 (1998).
[43] A. Venkatesan and M. Lakshmanan, Phys. Rev. E **63**, 026219 (2001).
[44] Y. Pomeau and P. Manneville, Commun. Math. Phys. **74**, 189 (1980).
[45] O. Sosnovtseva, U. Feudel, J. Kurths, and A. Pikovsky, Phys. Lett. A **218**, 255 (1996).
[46] S. Datta, R. Ramaswamy, and A. Prasad, Phys. Rev. E **70**, 046203 (2004).
[47] S.-Y. Kim, W. Lim, and E. Ott, Phys. Rev. E **67**, 056203 (2003).
[48] S. S. Negi, A. Prasad, and R. Ramaswamy, Physica D **145**, 1 (2000).
[49] T. Yalçinkaya and Y. C. Lai, Phys. Rev. E **56**, 1623 (1997).
[50] See, e.g., Fig. 7 in A. Prasad, S. S. Negi, and R. Ramaswamy, Int. J. Bifurcation Chaos Appl. Sci. Eng. **11**, 291 (2001).